Analyst

RSC Publishing

PAPER

View Article Online
View Journal | View Issue

Theoretical estimation of drag tag lengths for direct quantitative analysis of multiple miRNAs (DQAMmiR)†

Cite this: *Analyst*, 2013, **138**, 553

Leonid T. Cherney and Sergey N. Krylov*

To better understand the regulatory roles of miRNA in biological functions and to use miRNA as molecular markers of diseases, we need to accurately measure amounts of multiple miRNAs in biological samples. Direct quantitative analysis of multiple miRNAs (DQAMmiR) has been recently developed by using a classical hybridization approach where miRNAs are hybridized with fluorescently labeled complementary DNA probes taken in excess, and the amounts of the hybrids and the unreacted probes are measured to calculate the amount of miRNAs. Capillary electrophoresis was used as an instrumental platform for analysis. The problem of separating the unreacted probes from the hybrids was solved by adding SSB to the run buffer. A more difficult problem of separating hybrids from each other was solved by attaching different drag tags to the probes. Biotin and a hairpin-forming extension on the probe were used as two drag tags in the proof-of-principle work. Making DQAMmiR a generic approach requires a generic solution for drag tags. Peptides have been suggested as drag tags for long oligonucleotides in DNA sequencing by electrophoresis. Here we theoretically consider short peptides of different lengths as drag tags for DQAMmiR. We find analytical equations that allow us to estimate mobilities of RNA–DNA hybrids with peptide drag tags of different lengths. Our calculations suggest that the mobility shifts required for DQAMmiR can be achieved with the length of peptide chains in the ranges of 5–20 residues for five miRNAs and 2–47 residues for nine miRNAs. Peptides of these lengths can be feasibly synthesized with good yield and purity. The results of this theoretical study will guide the design and production of hybridization probes for DQAMmiR.

Received 11th September 2012
Accepted 2nd November 2012

DOI: 10.1039/c2an36296a

www.rsc.org/analyst

Introduction

MicroRNAs (miRNAs) are short, non-coding RNA molecules (18–26 nucleotides) that participate in the regulation of gene expression.[1] They can serve as diagnostic tools since altered expression patterns of multiple miRNAs have been linked to serious diseases including some forms of cancer.[2–4] Using miRNA in diagnostics requires quantitative analyses of multiple miRNAs. Most miRNA detection methods (quantitative reverse-transcriptase polymerase chain reaction, microarrays, surface plasmon resonance, next generation sequencing, *etc.*) are indirect and require chemical or enzymatic modifications of miRNA as a part of analysis.[5–8] Such modifications are complex and lead to a decrease in accuracy due to the influence of miRNA sequence on modification efficiency.[9–11] Conventional direct methods (northern blotting, signal amplifying ribozymes, *in situ* hybridization, bioluminescence detection, and two-probe single-molecule fluorescence) do not require any modification of the target miRNA, but they can provide only semi-quantitative analysis of multiple miRNAs.[12–16]

A method for direct quantitative analysis of multiple miRNAs (DQAMmiR) has been recently developed in our laboratory.[17] This method employs a hybridization approach in capillary electrophoresis (CE) with laser-induced fluorescence (LIF) detection (Fig. 1). Single stranded DNA (ssDNA) probes are labeled fluorescently for detection, taken in excess to miRNAs, and bind miRNAs sequence-specifically. Probes are also extended with drag tags of varying sizes, which results in different electrophoretic mobilities of probes and probe–miRNA hybrids. ssDNA binding protein (SSB) is added to the run buffer to separate the unreacted probes from the probe–miRNA hybrids.[18–21] The hybrids are separated from each other due to the drag tag induced differences in their mobilities. Peak areas corresponding to the unreacted probes and individual hybrids are measured and used in a simple algebraic formula to calculate absolute amounts of miRNAs. DQAMmiR is a calibration-free approach that promises robustness and ruggedness required for validation of miRNA disease signatures.

In the original work on DQAMmiR, we utilized two tagged probes and one untagged probe and thus could analyze 3 miRNAs in one assay. The drag tags were biotin and a DNA extension forming a hairpin. While satisfactory for

Department of Chemistry and Centre for Research on Biomolecular Interactions, York University, Toronto, Ontario M3J 1P3, Canada. E-mail: skrylov@yorku.ca; Fax: +1 416-736-5936; Tel: +1 416-736-2100 ext. 22345

† Electronic supplementary information (ESI) available. See DOI: 10.1039/c2an36296a

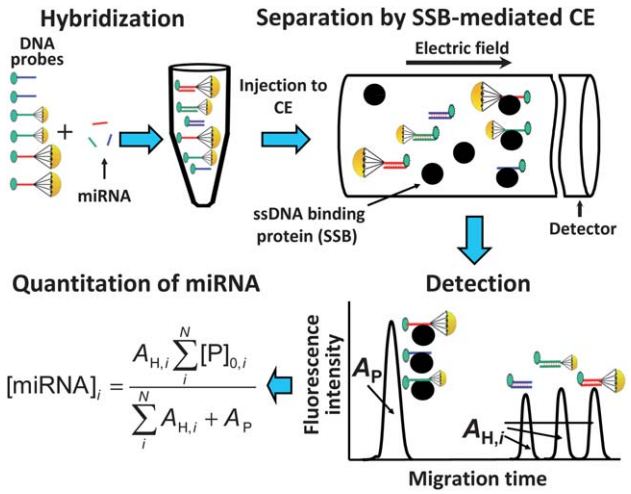

Fig. 1 Schematic representation of the direct quantitative analysis of multiple miRNAs by CE. MiRNAs and their complimentary ssDNA probes are shown as short lines of the same color, drag tags are shown as parachutes, a fluorescent label is shown as small green circles and ssDNA-binding protein (SSB) is shown as large black circles. In the hybridization step, an excess of the probes of concentrations $[P]_{0,i}$ is mixed with the miRNAs which leads to all miRNAs' being hybridized but with some probes left unbound. A short plug of the hybridization mixture is introduced into a capillary prefilled with a SSB-containing run buffer. SSB binds all ssDNA probes but does not bind the double stranded miRNA–DNA hybrid. When an electric field is applied, all SSB-bound probes move faster than all the hybrids (SSB works as a propellant).[18–21] Different drag tags make different hybrids that move with different velocities. A fluorescent detector registers signals from hybrids and unreacted probes. The amounts (or concentrations) of miRNAs are finally determined with a simple mathematical formula that uses the integrated signals (peak areas in the graph: $A_{H,i}$ for the areas corresponding to the hybrids and A_P for the total area corresponding to the unreacted probes). Adopted with permission from ref. 17. Copyright 2001 John Wiley and Sons, Inc.

proof-of-principle, these tags are not extendable and cannot support the analysis of >3 miRNAs. On the other hand, practical uses of DQAMmiR, such as for cancer profiling, will certainly require simultaneous analysis of >3 miRNAs. The next step in the development of DQAMmiR is to design an approach for generic expandable drag tags. Polymers of different lengths would work well for this purpose. Controlling the exact length in synthetic polymers is difficult. In peptides – natural polymers – the length is controlled by the number of residues and can be changed precisely. To choose the number of residues, one needs to know the ideal lengths of the peptide tags that allow for optimal separation. Generally speaking, appropriate lengths of peptides could be determined experimentally by trying their various combinations. Unfortunately, chemistry of peptide synthesis and its conjugation to DNA is not trivial and is expensive. Therefore, it is essential to theoretically estimate the range of peptide lengths required prior to screening the drag tags experimentally.

Peptides have been proposed as drag tags in electrophoresis-based DNA sequencing and some theoretical approaches have been developed for calculating the mobilities of DNA-peptide chimeras.[22–28] As we show in the Results and discussion section these approaches cannot be directly applied to short probe–miRNA hybrids studied in DQAMmiR. We thus modified the existing theoretical approaches and developed our own method for estimating the mobility of the tagged hybrids and probes. The method was used to determine the lengths of peptide drag tags in the analysis of 5 miRNAs (4 tagged and 1 untagged hybrids). Further, our estimates of hybrid separation from each other suggested that 9 miRNAs can be analyzed by using peptide drag tags with 0–47 residues. Synthesis of peptide tags within this range of lengths is feasible. Two important features of optimal drag tags were found: (i) the increments in peptide lengths should increase with increasing peptide length and (ii) the longer peptides should be attached to shorter ssDNA fragments. Our results justify experimental tests of the peptide drag tags in DQAMmiR and suggest the strategy of the drag tag design. The expandable drag tag will make DQAMmiR a practical tool for the analysis of multiple miRNAs.

Results and discussion

The goal of this theoretical consideration is to estimate the mobility shift induced by a peptide tag on an miRNA–ssDNA hybrid. The physics of electromigration and thus formulae used to describe it depend on the lengths of both the hybrid and the peptide tag. The length of the hybrid is limited to the narrow range of miRNA lengths: 18–26 nucleotides. As for the peptide drag tag, we first consider an example of 5–20 residues (in the case of five miRNAs) with the understanding that if suitable mobility shifts could not be achieved then we would consider longer peptides.

It is well known that even a low concentration of salt in a buffer decreases the Debye length λ_D to molecular sizes (λ_D = 1.1 nm for 25 mM Borax) and screens electrical charges of nucleotides. As a result DNA molecules behave like free-draining polymers and their migration becomes size-independent.[29] Peptides have been considered as tags allowing one to achieve a DNA mobility shift in CE mainly in application to DNA sequencing. Accordingly, the theory of end-labeled free-solution electrophoresis (ELFSE) of DNA has been developed.[22–27] However, the theory of ELFSE was developed for oligonucleotides significantly longer (hundreds of base pairs) than miRNAs. The theory uses an assumption that oligonucleotides behave as a semiflexible random coil.[25] Such an assumption cannot be made for short 18–26 nt long miRNA–ssDNA hybrids. Indeed, the assumption is valid if the polymer contour length $L = Nb$ is much larger than the Kuhn length b_K which can be used to characterize the polymer stiffness.[30,31] Here, N is the number of monomers and b is the monomer length. The condition $L \gg b_K$ is not satisfied in our case of maximum 26 nt hybrids (for which $N_{hyb} = 26$ and $b_{hyb} \approx 0.34$ nm) since we have $L_{hyb} = N_{hyb}b_{hyb} < 9$ nm whereas $b_{K,hyb} > 20$ nm, where the subscript 'hyb' shows that the corresponding parameters describe miRNA–ssDNA hybrids (see ESI†). Therefore, the theory of ELFSE is not applicable to our case. There are experimental studies on short ssDNA with drag tags attached, which use the ELFSE theory.[32–35] However, their results are not applicable to miRNA–ssDNA hybrids which are much less flexible than ssDNA.

Given that L_{hyb} is several times smaller than $b_{K,hyb}$, we adopt a different theoretical approach. We assume that the

miRNA–ssDNA hybrid behaves like a rigid rod moving parallel to its axis. The hybrid diameter, d_{hyb}, can be estimated to be 2.6 nm.[36,37] It is higher than the Debye length λ_D, and the hybrid length L_{hyb} is many times higher than λ_D. As a result, one could expect that the hybrid mobility, μ_{hyb}, is estimated by the size-independent expression used for a thin double layer[25,29]

$$\mu_{hyb} = \frac{\varepsilon_0 \varepsilon_r \zeta}{\eta} \approx \frac{\sigma \lambda_D}{\eta} \left(\zeta \approx E_s \lambda_D,\ E_s = \frac{\sigma}{\varepsilon_0 \varepsilon_r} \right) \quad (1)$$

here, ε_0 is the vacuum permittivity, ε_r is the relative permittivity of the buffer, ζ is the zeta potential, σ is the surface density of the electric charge in the diffuse part of the double layer around the miRNA–ssDNA hybrid (*i.e.* excluding the Stern layer), E_s is the electric field strength at the inner surface of the double layer, η is the dynamic viscosity of the buffer. However, the situation is complicated by the condensation of the counter ions on the hybrid.[38–40] This effect takes place for cylindrical objects carrying a sufficiently larger electric charge, Q,[38]

$$q = \frac{Q}{L_{hyb}} \geq q_{eff},\ q_{eff} = \frac{e}{z_i \lambda_B},\ \lambda_B = \frac{e^2}{4\pi \varepsilon_0 \varepsilon_r k_B T} \quad (2)$$

here, q is the linear density of the electric charge, e is the elementary charge, z_i is the valance of counter ions, λ_B is the Bjerrum length, T is the absolute temperature of the buffer, k_B is the Boltzmann constant. We assume that the electric charge is uniformly distributed along the hybrid length. For example, ssDNA usually has one negative charge per 0.43 nm of its length.[25] On the other hand, $\lambda_B = 0.7$ nm for water solutions at room temperature.[40] Therefore, condition (2) is always satisfied for miRNA–ssDNA hybrids. As a result, the condensation of counter ions reduces the density of the hybrid charge to the effective value, q_{eff}, determined by the second relation (2).[24,40] In this case, relation (1) for hybrid mobility can be rewritten as follows:

$$\mu_{hyb} = \frac{\sigma \lambda_D}{\eta} = \frac{q_{eff} \lambda_D}{\pi \eta d_{hyb}},\ \sigma = \frac{q_{eff}}{\pi d_{hyb}} \quad (3)$$

here, we consider the Stern layer as a part of the condensed counter ion layer. The expression (3) for σ takes into account the condensation of counter ions at $Q/L_{hyb} > q_{eff}$ where Q is the electric charge of the hybrid. Relations (3) also allow one to estimate the mobility μ_{DNA} of short DNAs. They lead to a value of $\mu_{DNA} = 3 \times 10^{-4}$ cm^2 V^{-1} s^{-1} which agrees with the previously published data.[25] Expression (3) for μ_{hyb} can also be obtained from the balance of electric and hydrodynamic forces, $F_{E,hyb}$ and $F_{H,hyb}$, acting upon the hybrid,

$$F_{E,hyb} = F_{H,hyb} \quad (4)$$

if we assume the following effective values for these forces:

$$F_{E,hyb} = q_{eff} L_{hyb} E,\ F_{H,hyb} = \frac{\pi \eta d_{hyb} L_{hyb}}{\lambda_D} u_{rel} \quad (5)$$

here, E is the electric field strength and u_{rel} is the relative velocity of the hybrid (with respect to the buffer). Expression (5) for $F_{H,hyb}$ differs by the coefficient C from the force $F^*_{H,hyb}$ acting upon the cylinder moving along its axis:[41]

$$F = CF^*_{H,hyb},\ F^*_{H,hyb} = 2\pi \eta L_{hyb} u \left(\ln \frac{2L_{hyb}}{d_{hyb}} - \frac{1}{2} \right)^{-1} \quad (6)$$

$$C = \frac{d_{hyb}}{2\lambda_D} \left(\ln \frac{2L_{hyb}}{d_{hyb}} - \frac{1}{2} \right) \quad (7)$$

If formula (6) for $F^*_{H,hyb}$ is used instead of $F_{H,hyb}$ in the equation for balance of electric and hydrodynamic forces (eqn (4)), then the corresponding expression for hybrid mobility μ^*_{hyb} will differ from μ_{hyb} also by coefficient C:

$$\mu^*_{hyb} = \frac{q_{eff}}{2\pi \eta} \left(\ln \frac{2L_{hyb}}{d_{hyb}} - \frac{1}{2} \right) = C\mu_{hyb} \quad (8)$$

We have $C = 1.5$ at $d_{hyb} = 2.6$ nm, $\lambda_D = 1.1$ nm, and $L_{hyb} = 8$ nm. An expression similar to (8) was applied by Desruisseaux *et al.* to estimate the ssDNA mobility, μ_{ssDNA}.[24] The authors used arguments that μ_{ssDNA} equals to the mobility of DNA fragments with length λ_D and width b.[24,40] Such an approach corresponds to an assumption $L_{hyb}/d_{hyb} = \lambda_D/b$ in our case, which also leads to $C = 1.5$. Thus, relations (5) and (6) give values of the same order ($F_{H,hyb}$ and $F^*_{H,hyb}$) for the hydrodynamic force, and relations (3) and (8) give values of the same order (μ_{hyb} and μ^*_{hyb}) for hybrid mobility.

The situation with the flexibility of our peptide drag tags is different. Their contour lengths, $L_{tag} = N_{tag} b_{tag}$, are greater than the Kuhn length of short peptides, $b_{K,tag}$, that is of the order of 1 nm.[42,43] Here, N_{tag} and b_{tag} are the number of residues in the peptide tag and the length of one residue. In this case, the drag tag size can be described by the gyration radius $R_{G,tag}$ that is determined by the Kratky–Porod equation (S2†) in terms of $b_{K,tag}$ and L_{tag} (see ESI†). Estimations give values $R_{G,tag} = 0.39$, 0.64, 0.83, and 0.99 nm for drag tags containing 5, 10, 15, and 20 residues, respectively. These values are significantly smaller than the length of the DNA–RNA hybrids and we can assume that the drag tag forms a worm-like chain located at the end of the miRNA–ssDNA hybrid.

The hydrodynamic force, $F_{H,tag}$, acting upon the drag tag is determined by expression

$$F_{H,tag} = 6\pi \eta R_{H,tag} u_{rel} \quad (9)$$

where $R_{H,tag}$ is the hydrodynamic radius of the drag tag. A value of $R_{H,tag}$ can be related to the gyration radius of drag tags:[44,45]

$$R_{G,tag} = \rho R_{H,tag} \quad (10)$$

where $\rho = 1.5$ for a Gaussian coil. In a more general case, ρ can be considered as a phenomenological parameter of the order of unity. Theoretical relation (10) gives values of 0.26, 0.43, 0.55, and 0.66 nm for the hydrodynamic radius of drag tags containing 5, 10, 15, and 20 residues, respectively (for $\rho = 1.5$).

The mobility $\mu_{hyb+tag}$ of the hybrid with the peptide drag tag attached can be found from the balance of all forces acting upon such a complex

$$F_{E,hyb} = F_{H,hyb} + F_{H,tag} \quad (11)$$

Substituting expressions (5) and (9) for $F_{E,hyb}$, $F_{H,hyb}$, and $F_{H,tag}$ into (11) and solving this equation with respect to the velocity, we finally obtain

$$u_{rel} = \mu_{hyb+tag}E,\ \mu_{hyb+tag} = \frac{\mu_{hyb}}{1 + \frac{6\lambda_D R_{H,tag}}{d_{hyb}L_{hyb}}} \quad (12)$$

here, L_{hyb} is directly proportional to the number of nucleotides in the hybrid, N_{hyb}. Dependence of $R_{H,tag}$ on the number of residues in the peptide tag, N_{tag}, is more complex and determined by relations (10) and (S2†) given that $L_{tag} = N_{tag}b_{tag}$. Fig. 2 shows how the relative mobility of the hybrid with the drag tag, $\mu_{rel} = \mu_{hyb+tag}/\mu_{hyb}$ depends on N_{tag} at various values of N_{hyb}. It should be emphasized that μ_{hyb} does not depend on N_{hyb}. Therefore, a pattern for the absolute mobility of the hybrid with the drag tag, $\mu_{hyb+tag}$, will be similar to the pattern shown in Fig. 2. All curves will start at the same point (0, μ_{hyb}) and then (with increasing N_{tag}) they will split in a way similar to the one shown in Fig. 2. As one could expect, the mobility decreases with increasing N_{tag} and this effect is more pronounced for shorter hybrids.

Using relations (10) for $R_{H,tag}$ we assume that the peptide attached to the hybrid is not deformed (in particular, not stretched out) by the hydrodynamic friction force acting upon it. Indeed, such a deformation could take place at values of $F_{H,tag}$ that can be estimated as follows:[23–25]

$$F_{H,tag} \sim \frac{k_B T}{R_{G,tag}} \quad (13)$$

Taking into account relations (9) and (12) for $F_{H,tag}$ and u_{rel}, we obtain the characteristic value of the electric field strength, E^*, at which the peptide deformation is possible:

$$E^* \sim \frac{k_B T}{6\pi\eta R_{H,tag}R_{G,tag}\mu_{hyb+tag}} \geq \frac{k_B T}{6\pi\eta R_{H,tag}R_{G,tag}\mu_{hyb}} \quad (14)$$

Given the hybrid mobility $\mu_{hyb} \sim 3 \times 10^{-4}$ cm^2 V^{-1} s^{-1} resulting from (3), relations (14) give $E^* \sim 70$ kV cm^{-1} at $R_{H,tag} \sim 1$ nm and $R_{G,tag} \sim 1$ nm. This value of E^* is much higher than the values of the electric field strength used in CE (<600 V cm^{-1}).

Expressions (12) allow one to easily calculate the travel time of the hybrid with the drag tag to the detector, t_{det},

$$t_{det} = \frac{L_{det}}{u} = \frac{L_{det}}{u_{EOF} - \mu_{hyb+tag}E}\ (u = u_{EOF} - \mu_{hyb+tag}E) \quad (15)$$

here, L_{det} is the travel distance to the detector, u_{EOF} is the velocity of the electroosmotic flow, u is the total velocity of the hybrid with the drag tag. We also took into account the fact that the hybrid charge is negative. For hybrids without drag tags one should use μ_{hyb} instead of $\mu_{hyb+tag}$ in relation (15). Fig. 3 shows dependencies of the travel time, t_{det}, determined by expression (15) on the number of residues in the drag tag N_{tag} at various numbers of nucleotides in the hybrid, N_{hyb}. Calculations were made for values $L_{det} = 40$ cm, $u_{EOF} = 0.25$ cm s^{-1}, $E = 500$ V cm^{-1} that are typical in CE studies of miRNAs.[17] The absolute mobility $\mu_{hyb+tag}$ was found from the second relation (12) with μ_{hyb} determined by expression (3) that results in $\mu_{hyb} = 3.1 \times 10^{-4}$ cm^2 V^{-1} s^{-1}. The travel time curves in Fig. 3 start at the same value of the travel time for all hybrids without the drag tag ($N_{tag} = 0$) and then split at $N_{tag} > 0$. An increase in N_{tag} leads to a decrease in the travel time since the hybrid with a longer drag tag has a smaller mobility and, therefore, migrates slower against the electroosmotic flow.

Expressions (12) and (15) for $\mu_{hyb+tag}$ and t_{det} along with Fig. 2 and 3 allow one to estimate shifts in the electrophoretic mobility and travel time caused by peptide tags as a function of the peptide length for hybrids of various lengths. Such information can help in choosing optimal lengths of peptide drag tags for multiple miRNAs. Let us consider as an example two scenarios of the drag tag distribution among five miRNAs of various lengths (Table 1). In the first scenario longer drag tags were attached to longer miRNAs. In contrast, in the second

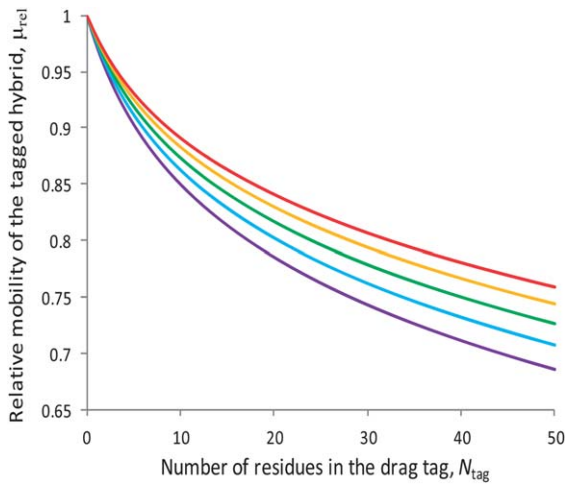

Fig. 2 Dependence of the relative mobility $\mu_{rel} = \mu_{hyb+tag}/\mu_{hyb}$ for a hybrid with the peptide drag tag on the number of residues in the peptide, N_{tag}, at various numbers of nucleotides in the hybrid, N_{hyb}. Magenta, blue, green, yellow, and red colors correspond to $N_{hyb} = 18$, 20, 22, 24 and 26, respectively.

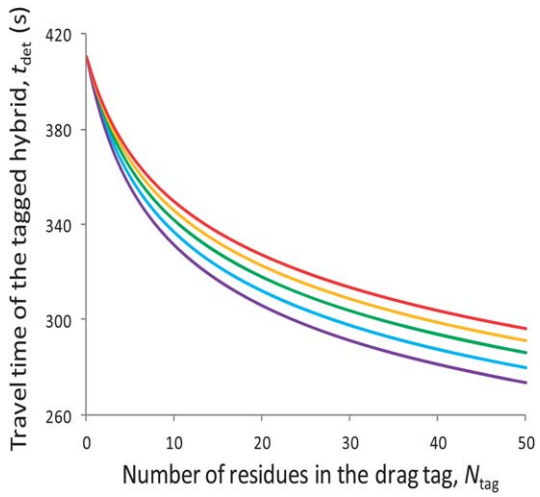

Fig. 3 Dependence of the travel time to the detector t_{det} for a hybrid with a peptide drag tag on the number of residues in the peptide, N_{tag}, at various numbers of nucleotides N_{hyb} in the hybrid. The color coding is the same as in Fig. 2.

Table 1 Relative mobility $\mu_{rel} = \mu_{hyb+tag}/\mu_{hyb}$ and travel time to the detector t_{det} for five hybrids with the peptide drag tags in the cases when the number of peptide residues, N_{tag}, increases and decreases with the number of nucleotides in the hybrid, N_{hyb}

	N_{tag} increasing with N_{hyb}			N_{tag} decreasing with N_{hyb}		
N_{hyb}	N_{tag}	μ_{rel}	t_{det}, s	N_{tag}	μ_{rel}	t_{det}, s
18	0	1.00	410	20	0.78	306
20	5	0.91	360	15	0.83	322
22	10	0.87	342	10	0.87	342
24	15	0.85	332	5	0.93	367
26	20	0.84	327	0	1.00	410

scenario longer drag tags were attached to shorter miRNAs. Values of μ_{rel} and t_{det} shown in Table 1 depend nonlinearly on N_{hyb} and N_{tag}, as it should be according to Fig. 2 and 3. Interestingly, the second scenario results in a larger average shift in μ_{rel} and t_{det} than the first one. Indeed, in the first scenario μ_{rel} and t_{det} span over ranges of 0.84–1 and 327–410 s, respectively, whereas these ranges increase to 0.78–1 and 306–410 s in the second scenario. The second scenario also leads to a more uniform distribution of shifts in μ_{rel} and t_{det} than the first scenario. Table 1 shows that the use of relatively short peptides as drag tags allows one to achieve at least 5% shift in the travel time to the detector among five hybrids. Such a shift is usually sufficient for distinguishing the corresponding peaks by CE.[17]

Eight peptides tags have to be used to separate nine miRNAs with N_{hyb} ranging from 18 to 26 nucleotides. Using expressions (12) and (15) we can choose lengths of the corresponding peptides and their distribution among probes to maintain 5% shift in t_{det} among all nine hybrids. The theoretical solutions derived from these expressions suggested that the optimal drag tag lengths for these miRNAs should consist of 2, 5, 9, 14, 20, 27, 36, and 47 amino acid residues. The corresponding probes are formed by attaching these peptides in a reverse order to ssDNA fragments the length of which increases monotonically. For example, the peptide with 47 residues is attached to 18 nt long ssDNA, the peptide with 36 residues is attached to 19 nt long ssDNA, and so on. Finally, there is no peptide attached to the 26 nt long ssDNA fragment. Two important features of the theoretically derived optimal drag tags should be noted: (i) increments in the peptide length grow with the increasing peptide length and (ii) the longer peptides are attached to shorter ssDNA fragments. The first feature follows from the steeper decline of the curves in Fig. 2 and 3 at smaller values of N_{tag} than at larger ones. The second feature reflects the fact that the curves in Fig. 2 and 3 which correspond to smaller values N_{hyb} are positioned lower than those corresponding to larger values of N_{hyb}. Thus, these features result from the qualitative behavior of curves in Fig. 2 and 3 and are not sensitive to quantitative estimates of mobilities and travel times of the hybrids. Of course, the found values of the peptide lengths (and corresponding values of t_{det}) may depend on such quantitative estimates. The described qualitative behavior of curves in Fig. 2 and 3 also explains the difference in the average shifts of μ_{rel} and t_{det} corresponding to the two scenarios shown in Table 1.

Relations (3) and (12) can be modified and applied to estimating the mobilities of unreacted probes and probes bound to SSB (see ESI†). It is also worth noting that the absolute evaluation of the electrophoretic mobility of short oligonucleotides is a difficult problem[29] and relations (3) and (S5†) should be treated as rough estimates. The mobility can be also expressed by relation (1) in terms of the zeta potential that is often considered as a phenomenological parameter.

Concluding remarks

Here we developed a simple method for estimating the lengths of the peptide drag tags that can be used in DQAMmiR. This method is based on theoretical expressions (3) and (12) for the mobilities μ_{hyb} and $\mu_{hyb+tag}$ of the untagged and tagged hybrids and on expression (15) for the tagged hybrid travel time to the detector t_{det}. Dependencies of $\mu_{hyb+tag}/\mu_{hyb}$ and t_{det} on the peptide and hybrid lengths were illustrated in Fig. 2 and 3. Expressions (3) and (12) were also modified for estimating the mobilities of unreacted probes and those bound to SSB (ESI†). As an example we considered the use of four drag tags with $N_{tag} = 5$, 10, 15, and 20 in studies of five miRNAs with $N_{hyb} =$ 18, 20, 22, 24, and 26 (Table 1). We compared the direct distribution of peptides among five probes (N_{tag} increasing with an increase in N_{hyb}) with the reversed one (N_{tag} decreasing with an increase in N_{hyb}) and showed that the reverse distribution leads to larger and more uniform shifts in the mobilities and travel times of the hybrids. Then we estimated the lengths of eight drag tags and their distribution among nine probes that are required for the analysis of all nine miRNAs with N_{hyb} ranging from 18 to 26. The optimal choice of the corresponding nine probes was found. This set of tags can provide 5% shift in the travel times of the hybrids, which is sufficient for CE analysis of multiple miRNAs. The obtained results will facilitate the application of DQAMmiR for analyses of multiple miRNAs.

Acknowledgements

This work was funded by the Natural Sciences and Engineering Research Council of Canada.

References

1 B. D. Aguda, Y. Kim, M. Piper-Hunter, A. Friedman and C. B. Marsh, *Proc. Natl. Acad. Sci. U. S. A.*, 2008, **105**, 19678–19683.
2 R. Visone, L. Z. Rassenti, A. Veronese, C. Taccioli, S. Costinean, B. D. Aguda, S. Volinia, M. Ferracin, J. Palatini, V. Balatti, H. Alder, M. Negrini, T. J. Kipps and C. M. Croce, *Blood*, 2009, **114**, 3872–3879.
3 G. A. Calin, C. D. Dumitru, M. Shimizu, R. Bichi, S. Zupo, E. Noch, H. Aldler, S. Rattan, M. Keating, K. Rai, L. Rassenti, T. Kipps, M. Negrini, F. Bullrich and C. M. Croce, *Proc. Natl. Acad. Sci. U. S. A.*, 2002, **99**, 15524–15529.

4 M. Z. Michael, S. M. O'Connor, N. G. van Holst Pellekaan, G. P. Young and R. J. James, *Mol. Cancer Res.*, 2003, **1**, 882–891.
5 K. Lao, N. L. Xu, V. Yeung, C. Chen, K. J. Livak and N. A. Straus, *Biochem. Biophys. Res. Commun.*, 2006, **343**, 85–89.
6 C.-G. Liu, G. A. Calin, B. Meloon, N. Gamliel, C. Sevignani, M. Ferracin, C. D. Dumitru, M. Shimizu, S. Zupo, M. Dono, H. Alder, F. Bullrich, M. Negrini and C. M. Croce, *Proc. Natl. Acad. Sci. U. S. A.*, 2004, **101**, 9740–9744.
7 S. Fang, H. J. Lee, A. W. Wark and R. M. Corn, *J. Am. Chem. Soc.*, 2006, **128**, 14044–14046.
8 R. D. Morin, M. D. O'Connor, M. Griffith, F. Kuchenbauer, A. Delaney, A.-L. Prabhu, Y. Zhao, H. McDonald, T. Zeng, M. Hirst, C. J. Eaves and M. A. Marra, *Genome Res.*, 2008, **18**, 610–621.
9 E. Ohtsuka, S. Nishikawa, R. Fukomoto, S. Tanaka, A. F. Markham, M. Ikehara and M. Sugiura, *Eur. J. Biochem.*, 1977, **81**, 285–291.
10 L. W. McLaughlin, E. Romaniuk, P. J. Romaniuk and T. Neilson, *Eur. J. Biochem.*, 1982, **125**, 639–643.
11 E. A. Weiss, G. M. Gilmartin and J. R. Nevins, *EMBO J.*, 1991, **10**, 215–219.
12 E. Vàrallyay, J. Burgyan and Z. Havelda, *Nat. Protoc.*, 2008, **3**, 190–196.
13 J. S. Hartig, I. Grune, S. H. Najafi-Shoushtari and M. Famulok, *J. Am. Chem. Soc.*, 2004, **126**, 722–723.
14 W. P. Kloosterman, E. Wienholds, E. de Bruijn, S. Kauppinen and R. H. A. Plasterk, *Nat. Methods*, 2006, **3**, 27–29.
15 K. A. Cissell, Y. Rahimi, S. Shrestha, E. A. Hunt and S. K. Deo, *Anal. Chem.*, 2008, **80**, 2319–2325.
16 L. A. Neely, S. Patel, J. Garver, M. Gallo, M. Hackett, S. McLaughlin, M. Nadel, J. Harris, S. Gullans and J. Rooke, *Nat. Methods*, 2006, **3**, 41–46.
17 D. W. Wegman and S. N. Krylov, *Angew. Chem., Int. Ed.*, 2011, **50**, 10335–10339.
18 M. Berezovski and S. N. Krylov, *J. Am. Chem. Soc.*, 2003, **125**, 13451–13454.
19 S. M. Krylova, D. Wegman and S. N. Krylov, *Anal. Chem.*, 2010, **82**, 4428–4433.
20 A. A. Al-Mahrouki and S. N. Krylov, *Anal. Chem.*, 2005, **77**, 8027–8030.
21 N. Khan, J. Cheng, J. P. Pezacki and M. V. Berezovski, *Anal. Chem.*, 2011, **83**, 6196–6201.
22 P. Mayer, G. W. Slater and G. Drouin, *Anal. Chem.*, 1994, **66**, 1777–1780.
23 S. J. Hubert and G. W. Slater, *Electrophoresis*, 1995, **16**, 2137–2142.
24 C. Desruisseaux, D. Long, G. Drouin and G. W. Slater, *Macromolecules*, 2001, **34**, 44–52.
25 R. J. Meagher, J.-I. Won, L. C. McCormick, S. Nedelcu, M. M. Bertrand, J. L. Bertram, G. Drouin, A. E. Barron and G. W. Slater, *Electrophoresis*, 2005, **26**, 331–350.
26 R. J. Meagher, L. C. McCormick, R. D. Haynes, J.-I. Won, J. S. Lin, G. W. Slater and A. E. Barron, *Electrophoresis*, 2006, **27**, 1702–1712.
27 D. Long, A. V. Dobrynin, M. Rubinstein and A. Ajdari, *J. Chem. Phys.*, 1998, **108**, 1234–1244.
28 C. Desruisseaux, G. Drouin and G. W. Slater, *Macromolecules*, 2001, **34**, 5280–5286.
29 J.-L. Viovy, *Rev. Mod. Phys.*, 2000, **72**, 813–872.
30 I. Teraoka, *Polymer Solutions*, John Wiley & Sons, New York, 2002, p. 360.
31 G. R. Strobl, *The Physics of Polymers: Concepts for Understanding Their Structures and Behavior*, Springer, Berlin, 2007, p. 518.
32 W. N. Vreeland, C. Desruisseaux, A. E. Karger, G. Drouin, G. W. Slater and A. E. Barron, *Anal. Chem.*, 2001, **73**, 1795–1803.
33 W. N. Vreeland, G. W. Slater and A. E. Barron, *Bioconjugate Chem.*, 2002, **13**, 663–670.
34 R. D. Haynes, R. J. Meagher, J.-I. Won, F. M. Bogdan and A. E. Barron, *Bioconjugate Chem.*, 2005, **16**, 929–938.
35 R. J. Meagher, J. A. Coyne, C. N. Hestekin, T. N. Chiesl, R. D. Haynes, J.-I. Won and A. E. Barron, *Anal. Chem.*, 2007, **79**, 1848–1854.
36 F. C. Simmel and W. U. Dittmer, *Small*, 2005, **1**, 284–299.
37 Y. Krishnan and F. C. Simmel, *Angew. Chem., Int. Ed.*, 2011, **50**, 3124–3156.
38 G. S. Manning, *J. Chem. Phys.*, 1969, **51**, 924–933.
39 G. S. Manning, *J. Phys. Chem.*, 1981, **85**, 1506–1515.
40 J. L. Barrat and J. F. Joanny, *Adv. Chem. Phys.*, 1996, **94**, 1–81.
41 J. Happel and H. Brenner, *Low Reynolds number hydrodynamics with Special applications to Particulate Media*, Springer, 1983, p. 553.
42 Y. Zhang and J. Skolnick, *Proc. Natl. Acad. Sci. U. S. A.*, 2005, **102**, 1029–1034.
43 F. Gräter, P. Heider, R. Zangi and B. J. Berne, *J. Am. Chem. Soc.*, 2008, **130**, 11578–11579.
44 W. Burchard, M. Schmidt and W. H. Stockmayer, *Macromolecules*, 1980, **13**, 1265–1272.
45 J. des Cloizeaux and G. Jannink, *Polymers in Solution: Their Modelling and Structure*, Clarendon Press, New York, 2010, p. 896.

Supporting Information

Estimation of drag-tag lengths for direct quantitative analysis of multiple miRNAs

Leonid T. Cherney and Sergey N. Krylov

1. Inapplicability of ELFSE to short probe-miRNA hybrids

The theory of ELFSE was developed for significantly long oligonucleotides that presumably behave as a semiflexible random coil.[1-6] The latter is true if the polymer contour length $L = Nb$ is much greater than the Kuhn length b_K of the polymer. Here, N is the number of monomers and b is the monomer length. The b_K value is often related to persistence length p ($p = b_K/2$ for semiflexible polymers described by the worm-like chain model), which is a measure of the polymer's stiffness.[7,8] We approximately have $b = 0.34$ nm and $b_K = 100$ nm for double stranded DNA (dsDNA).[5] The single stranded DNA (ssDNA) is much more flexible and is described by values $b = 0.43$ nm and $b_K = 6$ nm.[5] In particular, calculations of the mobility of ssDNA with an attached drag tag[5] is based on the theory of polyampholyte electrophoresis that itself was developed for long polymer chains adopting a Gaussian conformation.[9] Since miRNAs contain a small number of nucleotides (~ 18-26) we have to understand if the ELFSE theory can be applied to migration of DNA-miRNA duplexes with attached drag tags. Structural studies of DNA-RNA hybrids show that they form hybrid helixes.[10] Their conformation is intermediate between A- and B-forms of dsDNA but more resembles the A-form.[11-14] The persistence length of dsDNA can be estimated as 45-50 nm[15], which is in agreement with the Kuhn length ~ 100 nm.[5] Double stranded RNA (dsRNA) is stiffer than dsDNA and the persistence length of dsRNA helix is larger (65-80 nm) than that of dsDNA.[14,16] One could expect that **a** DNA-RNA hybrid has intermediate stiffness and its persistence length lies in a range of 50-75 nm. There are only a few experimental studies on the persistence length of DNA-RNA hybrids. They indicate that persistence lengths **can be** as low as 20 nm in some cases.[17,18] However, even such surprisingly low values are still higher than the contour length $L_{hyb} < 9$ nm of short hybrids containing 18-26 nucleotides that we deal with in this work. As a result, the assumption made in ELFSE that long oligonucleotides behave as semiflexible random coils, is not applicable to short DNA-RNA complexes. Rather, these short hybrids seem to behave like ridged rods.

2. Flexibility of short peptide drag tags

The Kuhn length of short peptides, $b_{K,tag}$, is of the order of 1 nm magnitude and the persistence length is just ~ 0.5 nm.[19-22] On the other hand, contour lengths of peptides used for example in **Table 1** (see main text) are 1.8, 3.6, 5.4, and 7.2 nm for drag tags containing 5, 10, 15, and 20 residues, respectively. These values are several times higher than the persistence length of peptides. Thus, the latter should take a more compact conformation that can be properly described by the gyration radius $R_{G,tag}$. In the case of long polymers with the number of

monomers $N_{tag} > N^*_{tag}$ calculations of $R_{G,tag}$ require taking into account the excluded volume. The critical value N^*_{tag} is determined by relation[1,5]

$$N^*_{tag} = \frac{b^3_{K,tag}}{b_{tag} d^2_{tag}} \tag{S1}$$

where d_{tag} is the diameter of the peptide, $b_{tag} = 0.36$ nm is the crystallographic length per residue. This value is slightly smaller than the dynamic value of $b_{tag} = 0.4$ nm that accounts for the internal degrees of freedom of the peptide.[23] For peptides formed by glycine, alanine, and threonine we have $d_{tag} < 0.24$ nm and, therefore, $N_{tag}^* > 48$ that is larger than the number of residues in the drag tags used in this study. Thus we can neglect the effect of excluded volume on interactions in peptides. In this case, the gyration radius is determined by the Kratky-Porod equation[7,8]

$$R^2_{G,tag} = \frac{b_{K,tag} L_{tag}}{6}\left[1 - 3\left(\frac{b_{K,tag}}{2L_{tag}}\right) + 6\left(\frac{b_{K,tag}}{2L_{tag}}\right)^2 - 6\left(\frac{b_{K,tag}}{2L_{tag}}\right)^3\left(1 - \exp\left(-\frac{2L_{tag}}{b_{K,tag}}\right)\right)\right] \tag{S2}$$

where $L_{tag} = N_{tag}\, b_{tag}$ is the contour length of the peptide. For example, the gyration radii of drag tags containing 5, 10, 15, and 20 residues are 0.39, 0.64, 0.83, and 0.99 nm, respectively. These values are significantly smaller than the length of the ssDNA-miRNA hybrids and we can assume that the drag tag forms a worm-like chain located at the end of the ssDNA-miRNA hybrid.

The hydrodynamic radius of the drag tag, $R_{H,tag}$, can be related to the gyration radius of polymers by equation (10) (hereafter equation numbers without S refer to the main text). On the other hand, studies of unfolded proteins result in the following dependence for the hydrodynamic radius (in nm):[24]

$$R_{H,tag} = (0.22 \pm 0.11) N_{tag}^{0.57 \pm 0.02} \tag{S3}$$

that was obtained by fitting experimental data. Here, N_{tag} is the number of residues in the peptide chain. Expression (S3) gives approximately twice higher values for $R_{H,tag}$ (0.55, 0.82, 1.03, and 1.21 nm for drag tags containing 5, 10, 15, and 20 residues, respectively) than those found from (10). However, the order of magnitude of $R_{H,tag}$ remains the same.

3. Mobility of unreacted probes and probes bound to SSB

For ssDNA b_K = 6 nm[5] and is comparable to the length of ssDNA section (8 – 11 nm) in the probe. Thus, relation (3) can be used to estimate the mobility of ssDNA without a drag tag. In this case, a value of d_{hyb} present in (3) should be replaced with the diameter of ssDNA, d_{ssDNA}. The latter can be estimated as $d_{hyb}/2$[25,26] or can be considered as an adjustable parameter. The probe mobility can then be evaluated using the second relation (12) if μ_{hyb}, L_{hyb}, and d_{hyb} are replaced with μ_{ssDNA}, L_{ssDNA} and d_{ssDNA}, respectively. After such modification relation (12) will depend on the numbers of monomers in ssDNA, N_{DNA}, and in the tag, N_{tag}, through the ratio $R_{G,tag}(N_{tag})/N_{DNA}$ (since $L_{ssDNA} \sim N_{DNA}$), where function $R_{G,tag}(N_{tag})$ is determined by the Kratky-Porod equation (S2). The averaging procedure employed in ELFSE leads to a different dependence of the probe mobility on the ratio N_{tag}/N_{DNA}:

$$\mu_{ssDNA+tag} = \mu_{ssDNA}\left(1+\alpha\frac{N_{tag}}{N_{DNA}}\right)^{-1}, \quad \alpha = \frac{b_{tag}b_{K,tag}}{b_{ssDNA}b_{K,ssDNA}} \tag{S4}$$

Here, b_{ssDNA} and $b_{K,ssDNA}$ are the monomer size and the Kuhn length of ssDNA, respectively. Though the second relation (12) (modified for probes, i.e. for ssDNA with a tag) gives different dependencies of $\mu_{ssDNA+tag}/\mu_{ssDNA}$ on N_{DNA} and N_{tag} than the first relation (S4) does, these relations lead to close values in our ranges of N_{DNA} and N_{tag}. For example, at N_{DNA} = 20 and N_{tag} = 20 we obtain $\mu_{ssDNA+tag}/\mu_{ssDNA}$ = 0.72 and 0.87, respectively, from relations (12) (modified for probes) and (S4). Since $d_{ssDNA} < d_{hyb}$, we always have $\mu_{ssDNA} > \mu_{hyb}$. The mobility of the probe (i.e. $\mu_{ssDNA+tag}$) is also larger than that of the tagged hybrid.

Finally, let us consider the mobility of the probe bound to SSB, $\mu_{probe+SSB}$. SSB is a globular protein consisting of 177 residues and having the characteristic size ~ 10 nm. ssDNA bound to a SSB surface can be assumed to have a length <10 nm and a diameter ~1 nm. As a result, we can consider a complex of ssDNA-SSB as a globular object with approximately the same diameter ($d_{comp} \sim 10$ nm), as the native protein. In this case, its mobility, $\mu_{ssDNA+SSB}$ can be estimated by relations similar to equations (3)

$$\mu_{ssDNA+SSB} = \frac{\sigma_{ssDNA+SSB}\lambda_D}{\eta} = \frac{Q_{ssDNA+SSB}\lambda_D}{\pi\eta d_{SSB}^2} \quad \left(\sigma_{ssDNA+SSB} = \frac{Q_{ssDNA+SSB}}{\pi d_{SSB}^2}\right) \tag{S5}$$

Where $\sigma_{ssDNA+SSB}$ is the surface density of the electric charge in the diffuse part of the double layer around the complex of SSB and ssDNA, $Q_{ssDNA+SSB}$ is the total charge of this complex, and we neglected the Stern layer around the complex. Given the relatively small number of residues in the drag tag we can assume that $\mu_{probe+SSB} \approx \mu_{ssDNA+SSB}$. For much longer drag tags a relation for $\mu_{probe+SSB}$ can be derived similarly to relation (12) for $\mu_{hyb+tag}$. Indeed, an expression (S5) can be derived from the balance of electric and hydrodynamic forces, $F_{E,ssDNA+SSB}$ and $F_{H,ssDNA+SSB}$,

acting upon the ssDNA-SSB complex if we assume the following expressions for them (similarly to (5)):

$$F_{\mathrm{E,ssDNA+SSB}} = Q_{\mathrm{ssDNA+SSB}} E, \quad F_{\mathrm{H,ssDNA+SSB}} = \frac{\pi \eta d_{\mathrm{SSB}}^2}{\lambda_{\mathrm{D}}} u \tag{S6}$$

Then the mobility $\mu_{\mathrm{probe+SSB}}$ of the probe bound to SSB and having the long drag tag can be found from the balance of all forces acting upon such complex:

$$F_{\mathrm{E,ssDNA+SSB}} = F_{\mathrm{H,ssDNA+SSB}} + F_{\mathrm{H,tag}} \tag{S7}$$

Substituting expressions (S6) into equation (S7) and taking into account relation (9) we obtain

$$\mu_{\mathrm{probe+SSB}} = \frac{\mu_{\mathrm{ssDNA+SSB}}}{1 + \dfrac{6\lambda_{\mathrm{D}} R_{\mathrm{H,tag}}}{d_{\mathrm{SSB}}^2}} \tag{S8}$$

Here, the hydrodynamic radius of the drag tag, $R_{\mathrm{H,tag}}$, is determined by relations (10) and (S2). For short drag tags with $6\lambda_{\mathrm{D}} R_{\mathrm{H,tag}} << d^2_{\mathrm{SSB}}$ expression (S8) is reduced to $\mu_{\mathrm{probe+SSB}} \approx \mu_{\mathrm{ssDNA+SSB}}$.

References

1. Viovy, J.-L. *Rev. Modern Phys.* **2000**, *72*, 813-872.
2. Mayer, P.; Slater, G. W.; Drouin, G. *Anal. Chem.* **1994**, *66*, 1777-1780.
3. Hubert, S. J.; Slater, G. W. *Electrophoresis* **1995**, *16*, 2137-2142.
4. Desruisseaux, C.; Long, D.; Drouin, G.; Slater, G. W. *Macromolecules* **2001,** *34,* 44-52.
5. Meagher, R. J.; Won, J. - I.; McCormick, L., C.; Nedelcu, S.; Bertrand, M. M.; Bertram, J. L.; Drouin, G.; Barron, A., E.; Slater, G. W. *Electrophoresis* **2005**, *26*, 331-350.
6. Meagher, R. J.; McCormick, L., C.; Haynes, R. D.; Won, J. - I.; Lin, J. S.; Slater, G. W.; Barron, A. E. *Electrophoresis* **2006**, *27*, 1702-1712.
7. Teraoka, I. *Polymer Solutions* John Wiley & Sons, New York **2002**, 360 pp.
8. Strobl, G. R. *The physics of polymers: concepts for understanding their structures and behavior*, Springer, Berlin, **2007**, 518 pp.
9. Long, D.; Dobrynin, A. V.; Rubinstein, M.; Ajdari, A. *J. Chem. Phys.* **1998**, *108*, 1234-1244.
10. Rich, A. *J. Biol. Chem.* **2006**, *281*, 7693-7696.

11. Milman, G.; Langridge, R.; Chamberlin, M. J.; *Proc. Natl. Acad. Sci. U.S.A* **1967**, *57*, 1804-1810.
12. Lesnik, E. A.; Freier, S. M. *Biochemistry* **1995**, *34*, 10807-10815.
13. Fedoroff, O. Yu.; Salazar, M.; Reid, B. R. *J. Mol. Biol.* **1993**, *233*, 509-523.
14. Noy, A.; Pérez, A.; Márquez, M.; Luque, F. J.; Orozco, M. *J. Am. Chem. Soc.* **2005**, *127*, 4910-4920.
15. Cheatham, T. E., III; Kollman, P. A. *J. Mol. Biol.* **1966**, *259*, 434-444.
16. Kebbekus, P.; Draper, D. E.; Hagermad, P. *Biochemistry* **1995**, *34*, 4354-4357.
17. Wen, J.-D.; Manosas, M.; Li, P. T. X.; Smith, S. B.; Bustamante, C.; Ritort, F.; Tinoco, I., Jr. *Biophys. J.* **2007**, *92*, 2996-3009.
18. Collin, D.; Ritort, F., Jarzynski, C.; Smith, S. B.; Tinoco, I., Jr.; Bustamante, C. *Nature* **2005**, *437*, 231-234.
19. Hanke, F.; Serr, A.; Kreuzer, H. J.; Netz, R. R. *EPLA*, **2010**, *92*, 53001_p1-53001_p6.
20. Zhang, Y.; and Skolnick, J. *Proc. Natl. Acad. Sci. U.S.A.* **2005**, *102*, 1029-1034.
21. Rawat, N.; and Biswas, P. *J. Chem. Phys*. 2009, 131, 165104_1-165104_9.
22. Gräter, F.; Heider, P.; Zangi, R.; Berne, B. J. *J. Am. Chem. Soc*. **2008**, *130*, 11578–11579.
23. Ainavarapu, S. R. K.; Brujic, J.; Huang, H. H.; Wiita, A. P.; Lu, H.; Li, L.; Walther, K. A.; Carrion-Vazquez, M.; Li, H.; Fernandez, J. M. *Biophys. J.* **2007**, *92*, 225–233.
24. Wilkins, D. K.; Grimshaw, S. B.; Receveur, V.; Dobson, C. M.; Jones, J. A.; and Smith, L. J. *Biochemistry* **1999,** *38,* 16424-16431.
25. Simmel, F. C.; Dittmer, W. U. *Small* **2005**, *1*, 284-299.
26. Krishnan, Y.; Simmel, F. C. *Angew. Chem. Int. Ed.* **2011**, *50*, 3124–3156.